eng

MDPI

Article

Ultrasonically Accelerated Nitration of Hydroxyl-Terminated Polybutadiene: Process Efficiency and Product Characterization

Ventsislav Bakov [1], Spaska Yaneva [2], Nadezhda Rangelova [2], Milko Berner [3], Damyan Ganchev [4] and Nikolai Georgiev [1,*]

[1] Department of Organic Synthesis, University of Chemical Technology and Metallurgy, 8 Kliment Ohridsky Str., 1756 Sofia, Bulgaria; bakov@uctm.edu
[2] Department of Industrial Safety, University of Chemical Technology and Metallurgy, 8 Kliment Ohridsky Str., 1756 Sofia, Bulgaria; sp_yaneva@uctm.edu (S.Y.); rangelova@uctm.edu (N.R.)
[3] Department of Explosive Technique and Technologies, University of Mining and Geology "St. Ivan Rilski", Prof. Boyan Kamenov Str., 1700 Sofia, Bulgaria; m.berner@mgu.bg
[4] Department of Machine Elements and Non-Metal Constructions, Technical University, 11 Professor Georgi Bradistilov Str., 1756 Sofia, Bulgaria; ganchev_d@tu-sofia.bg
* Correspondence: nikigeorgiev@uctm.edu

Abstract

Hydroxyl-terminated polybutadiene (HTPB) is widely studied and the most used prepolymer for the binder system of composite solid propellants. A suitable functionalization of HTPB with energetic groups greatly improves the performance of the propellant. Therefore, the nitration of HTPB plays an essential role in the obtaining of high-energy binders. Among the reported methods, the nitration of HTPB using nitryl iodide (NO_2I) was distinguished as the most preferable due to the facilitated synthesis and product purity. However, the thus established synthesis is long and laborious; therefore, in the present work we focus our attention on the improved procedure using ultrasonic conditions. The resulted nitro-HTPB was characterized using FTIR, ^{1}H NMR, GPC, and DSC analyses. Also, based on the recorded IR-spectra a ratiometric analysis for determining the nitration rate was established, which could replace the expensive and time-consuming NMR analysis that was used.

Keywords: nitration; HTPB; ultrasonic activation; energetic binders; Fourier-transform infrared spectroscopy (FTIR)

Academic Editor: George Z. Papageorgiou

Received: 29 November 2025
Revised: 26 December 2025
Accepted: 28 December 2025
Published: 1 January 2026

1. Introduction

Hydroxyl-terminated polybutadiene (HTPB) has been one of the most widely used binders for composite solid propellants for several decades, valued for its excellent mechanical properties, low cost, ease of processing, and compatibility with a broad range of oxidizers, explosives, and metallic fuels [1–4]. Initially employed in composite rocket propellants, it is now utilized across a wide spectrum of composite energetic materials [5–9]. Conventional HTPB, however, is essentially non-energetic. It functions effectively as a binder, fuel, and structural matrix but contributes minimally to the overall energetic output of the formulation. This limitation has stimulated sustained interest in energetic binder systems, capable of simultaneously providing mechanical integrity and enhancing propellant performance.

Among the various existing options, nitrated HTPB stands out as a promising choice due to its structural similarity to conventional HTPB, which facilitates its integration into

established manufacturing processes while simultaneously providing a substantial increase in the energetic content of the binder [1,2,10–12]. The nitration process introduces nitro (-NO_2) and nitrate ester (-O-NO_2) functionalities into the polybutadiene chain, thereby improving the oxygen balance and increasing the energy density of the polymer [13–15]. As a result, nitrated HTPB exhibits a significantly higher heat of combustion and a more favorable oxygen balance than unmodified HTPB, enabling theoretical specific impulse increases of approximately 10–30 s depending on the oxidizer system and formulation [1,16]. This improvement may reduce required oxidizer content, increase payload capacity, or allow more compact motor design. Furthermore, nitration increases polymer density from approximately 0.9 g/cm^3 to 1.2–1.3 g/cm^3, contributing to higher overall energetic material density and improved volumetric energy characteristics—an essential valuable feature under stringent volume constraints [2,17].

Another notable advantage of nitrated HTPB is the retention of many desirable mechanical properties of conventional HTPB. Because nitrated HTPB is derived directly from HTPB, it can preserve elasticity toughness, and strong adhesion to solid fillers. With appropriate control of the nitration degree and curing conditions, nitrated HTPB-based propellant matrices can exhibit mechanical characteristics comparable to, or in some cases superior to, those obtained with conventional binders. Owing to these properties, nitrated HTPB is considered a promising material for a variety of advanced propulsion and energetic applications. Potential areas of use include solid rocket motors, where increased specific impulse and volumetric efficiency translate directly into improved range and payload of the rocket; orbital maneuvering motors that require high performance within strict geometric constrains; divert and attitude control systems; and gas generators and various CAD/PAD devices [16]. Nitrated HTPB is also relevant for low-signature propellants when paired with nitramine oxidizers or phase-stabilized ammonium nitrate, for insensitive munitions where performance must be balanced with safety, and for plastic-bonded explosives [1,16].

Despite these advantages, several challenges have limited the widespread adoption of nitrated HTPB. Traditional nitration methods are highly exothermic and rely on hazardous acidic media, creating significant safety and scale-up concerns. Controlled and inherently safer approaches, such as continuous-flow nitration, have recently emerged as promising alternatives. These techniques generally offer improved thermal management, reduced by-product formation, enhanced operational safety, and superior reaction reproducibility compared with conventional batch nitration [18,19]. Additionally, nitrated HTPB often exhibits higher intrinsic viscosity than standard HTPB at comparable molecular weight, complicating mixing and casting operations. Consequently, optimizing both the molecular weight distribution and the functionalization pattern is essential to achieving improved processability without compromising energetic performance [17].

Advances in synthesis technology therefore play a crucial role in overcoming these limitations. Modern strategies increasingly emphasize not only chemical modification but also process intensification and the development of robust processing methodologies. The overarching goal is to produce consistent and high-quality energetic binders with well-defined properties suitable for reliable large-scale manufacturing [16,18]. Continuous-flow nitration meets many of these requirements; however, its implementation is hindered by the need for complex expensive equipment and instrumentation and has limited applicability in the context of HTPB.

The chemistry of nitro compounds has been intensively explored during the last three decades. Various reaction pathways for the nitration of HTPB have been reported [20–25]. The most popular methods include the use of fuming nitric acid, nitrogen monoxide, nitryl iodide, nitromercuration–demercuration ($HgCl_2$-$NaNO_2$), and epoxidation and subsequent nitration with N_2O_5 in dichloromethane. Among them, due to the facilitated synthesis,

the product purity, the non-destructive nature, and the relatively low toxicity of the nitrating agent, while retaining the properties of starting olefin, the nitration of HTPB using nitryl iodide (NO_2I) stands out as a preferable approach for obtaining nitro-functional HTPB [26–29]. In this synthesis, nitryl iodide is formed in situ by the interaction of $NaNO_2$ and iodine, which attacks HTPB double bonds and gives the desired nitro derivative after subsequent elimination of HI from the formed nitro-iodo intermediate. However, the thus established procedure is long and laborious; therefore, in the present work we focus our attention on an improved procedure employing ultrasonic conditions.

The aim of the present study is to investigate the influence of the ultrasonication on both the efficiency and the rate of the nitration process conducted via the classical batch method, as well as to assess the properties of the resulting nitro-HTPB.

2. Materials and Methods

2.1. Materials

A Krasol LBH5000 (Cray Valley, Saint-Avold, France) was used as a starting HTPB. The commercially available sodium hydrogencarbonate, sodium nitrate, iodine, sodium sulphate, and sodium thiosulphate were purchased from Sigma-Aldrich (St. Louis, MO, USA) and were used without purification. The solvents used in the synthetic procedures ethylene glycol and ethyl acetate (Fisher Scientific, Waltham, MA, USA) were of pure and extra-pure grade, respectively.

2.2. Methods

The FTIR spectra were recorded on a Thermo Nicolet iS50 infrared spectrometer (Thermo Fisher Scientific, Waltham, MA, USA) with a diamond crystal ATR accessory at a resolution of 2 cm^{-1} and 64 scans. The spectra were referenced to air as a background by accumulating 64 scans, at the same resolution. The ^1H NMR spectra were acquired at room temperature (303 K) using a Bruker Avance 400 MHz spectrometer (Billerica, MA, USA) using $CDCl_3$ as the solvent. Chemical shifts (δ) are reported in parts per million (ppm). The average molecular weights were determined by GPC analysis on a Shimadzu Nexera XR (Shimadzu, Kyoto, Japan). The DSC studies were performed on a Mettler Toledo TA3000 thermal analysis system—DSC30 cell (Mettler Toledo, Columbus, OH, USA). The ultrasonic synthesis was performed in a BANDELIN SONOREX RK 100 H Ultrasonic Bath (Bandelin electronic gmbh & co. kg, Berlin, Germany). The ultrasonic power dissipated in the reaction mixture was determined calorimetrically by measuring the initial temperature rise of the solvent under identical experimental conditions. The effective acoustic power was 12 ± 3 W. The ultrasonic frequency was 35 kHz.

2.3. Synthetic Procedure

In a 1 L round-bottomed flask were dissolved 30.6 g HTBP (6 mmol) in 360 mL ethyl acetate. Then a solution of 26.5 g $NaNO_2$ (312 mmol) in 18 mL ethylene glycol and 42 mL water was added. The reaction mixture thus prepared was cooled to 0 °C and 36.6 g iodine (144 mmol) was added under vigorous stirring. After iodine addition the flask was placed in an ultrasonic bath for 25 h. Then the organic layer was separated and washed with 10% sodium thiosulphate until discoloration, followed by saturated aqueous $NaHCO_3$. The obtained organic solution was dried with anhydrous Na_2SO_4 and evaporated to give the crude product. The desired nitro-functional HTPB was obtained as a red-brown viscous liquid after washing with methanol to remove soluble impurities.

The chemical structure of the obtained product was confirmed by FTIR and ^1H NMR analysis. FTIR (ATR): 3500–3200 (br.s. νOH), 2922 and 2845 (νCH), 1640 (νCH=CH),

1523 and 1335 cm^{-1} (νNO_2). ^1H NMR: (400 MHz, $CDCl_3$) 7.2–6.9 (NO_2-C*H*-), 5.7–5.1 (-C*H*=), 5.1–4.8 (=CH_2), 2.3–1.8 (-CH_2- and CH-), and 1.05–1.0 (CH_2).

3. Results

The synthetic rout used herein is summarized in Scheme 1.

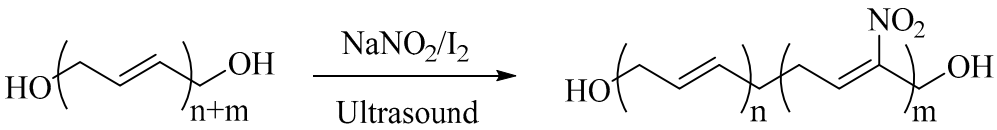

Scheme 1. Synthesis of nitro-functional HTPB.

Ethyl acetate was used as a solvent for HTPB, and a mixture of water and ethylene glycol was needed to dissolve the sodium nitrite. The two solutions were mixed and under vigorous stirring iodine was added to the mixture at 0 °C. Then the reaction vessel was placed in an ultrasonic bath for 25 h. After the end of the reaction, with the help of a separating funnel, the organic layer was subsequently separated and washed with sodium thiosulfate until it became decolorized. The final product was obtained in the form of a viscous liquid of nitro-functional HTPB after evaporation of the solvent under vacuum. The duration of the synthetic process was established using FTIR spectroscopy (a detailed explanation can be found below). The chemical functionalization of the obtained product was confirmed according to FTIR and ^1H NMR analyses.

The FTIR spectra are consistent with previous reports on nitro-HTPB and clearly indicate that the nitration does not affect the double bonds and hydroxyl groups in the initial HTPB. As can be seen in Figure 1, in contrast to the starting HTPB, the FTIR spectrum of nitro-functionalized product showed well-pronounced peaks at 1523 cm^{-1} and 1335 cm^{-1}, which are characteristic of asymmetric and symmetric stretch of α,β-unsaturated nitro olefine hydrocarbons [25,29]. In the range of 3500–3200 cm^{-1} the FTIR spectra of both compounds exhibited a very similar broad shoulder that could be attributed to the presence of hydroxyl groups in the HTPB backbone. The peak for alkene fragments in HTPB appeared at 1640 cm^{-1} and remained constant after nitro functionalization in the final product.

Also, the FTIR analysis was used to monitor and determine the completion of the nitration process. For this purpose, during the synthesis several 2 mL samples from the reaction mixture were taken and nitro-functional HTPB was isolated according to the method described above. Then the FTIR spectra of the obtained samples were recorded and are summarized in Figure 2.

In order to study the nitration rate while avoiding the effect of varying spectral baseline, the changes in intensity at 1523 cm^{-1} corresponding to asymmetric stretch of nitro groups in HTPB were inspected as a ratio to the constant alkenes signal at 1640 cm^{-1}. The observed results presented in Figure 2 reveal a sigmoidal fit (R^2 = 0.9984) with rapid linear increase during the first 10 h, suggesting fast nitration in the HTPB functionalization. After the first 10 h, the rate of increase gradually slowed and plateaued at 20 h, indicating completion of the HTPB nitration process. Thus, the duration of the ultrasonic synthetic route proposed herein is 20 h. This observation demonstrates a significant improvement in terms of reaction time compared to previously reported works on HTPB nitro functionalization using nitryl iodide in which the reaction time varies from 96 h to 144 h [28]. The accelerating ultrasonic effect could be explained according to two major factors: first, the ultrasound brings an additional amount of energy; second, it provides better mixing and a better contact surface in the used heterogeneous reaction, where sodium nitrite was dissolved in water and HTPB in water-immiscible ethyl acetate.

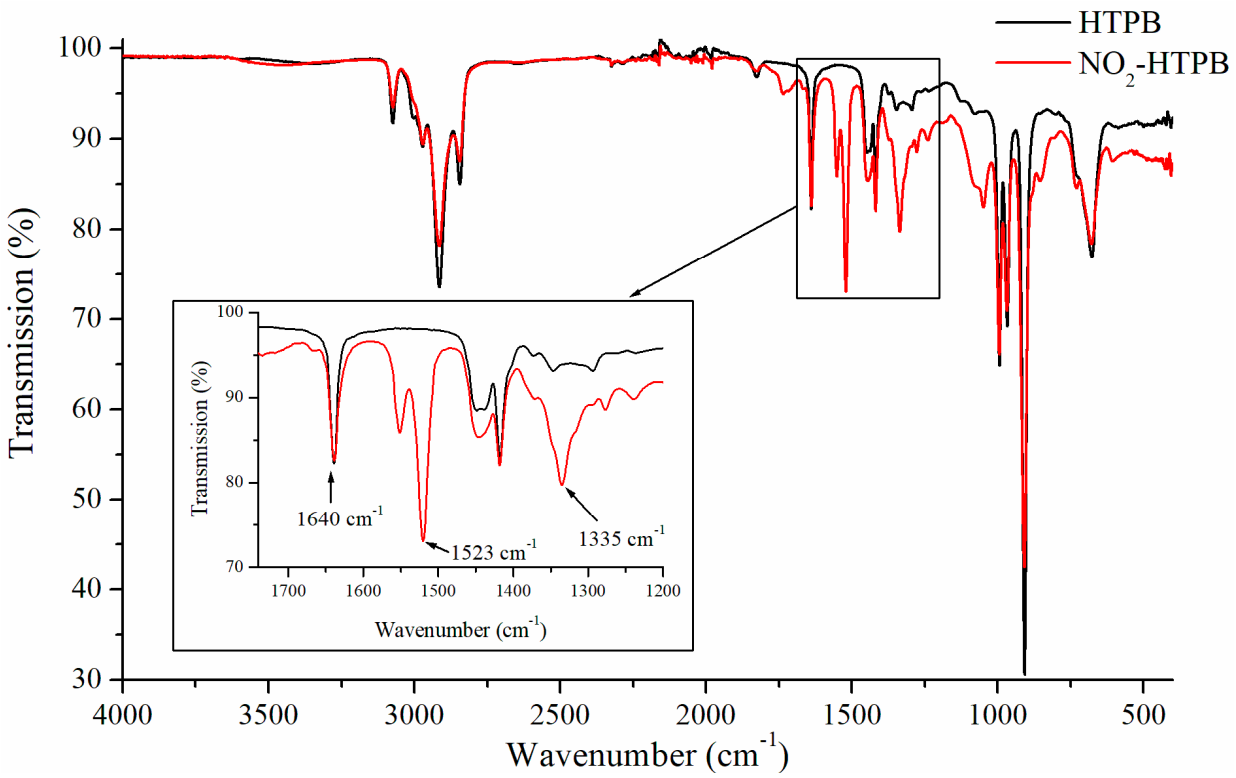

Figure 1. FTIR spectra of initial HTPB and synthesized nitro-functional product.

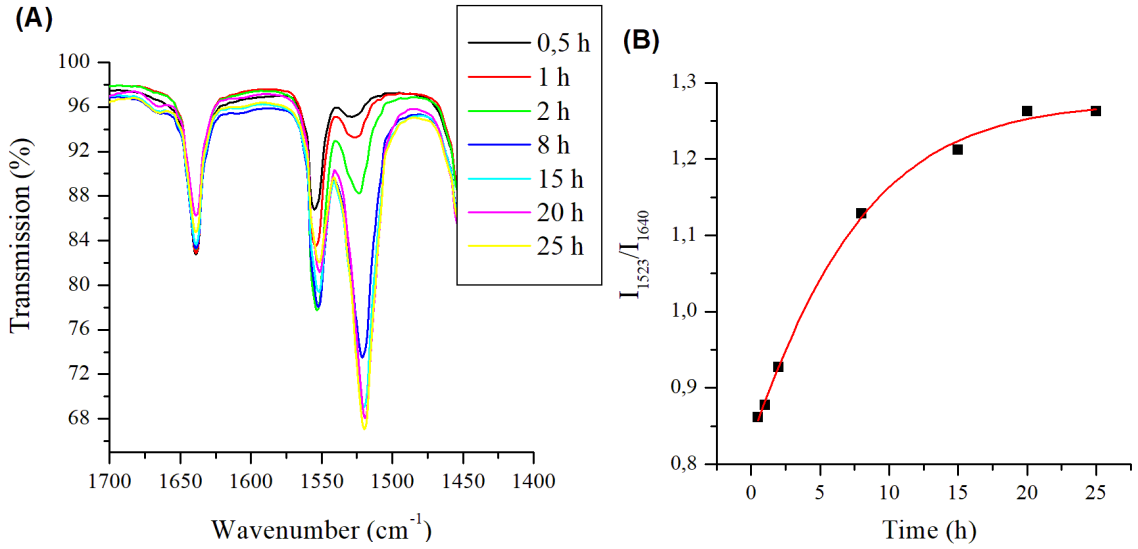

Figure 2. Changes in FTIR spectra of nitro-functional HTPB (**A**) and changes in ratio between intensity at 1523 cm^{-1} and constant alkenes signal at 1640 cm^{-1} (**B**) according to nitration time.

The observed ^{1}HNMR spectrum (Figure 3) of the synthesized nitro-HTPB was in accordance with previously reported data. Similarly to the starting HTPB it showed resonances in the range of 5.7–5.1 ppm and 5.1–4.8 attributed to -CH= and =CH_2 protons, respectively, and two resonance peaks in the range of 2.3–1.8 ppm and 1.5–1.0 ppm characteristic of -CH_2- and -CH- [30]. However, in the spectrum of nitrated HTPB, a novel peak in the range of 7.2–6.9 ppm appeared, which is a typical signal of protons from the NO_2-CH= groups. Due to the strong electron-accepting properties of the NO_2 group, a pronounced de-shielding effect occurs, causing the neighboring C–H proton to resonate at a higher frequency (higher ppm value) in the NMR spectrum. This large difference and lack of an overlap between the resonances of nitrated and non-nitrated olefin protons allow the use

of NMR analysis to determine the level of double-bond nitro functionalization. The level of 12% was calculated as follows: nitro functionalization % = 2×A/B + C, where A is the integral in the range of 7.2–6.9 ppm, while B and C are the integrals at 5.7–5.1 ppm and 5.1–4.8 ppm [28].

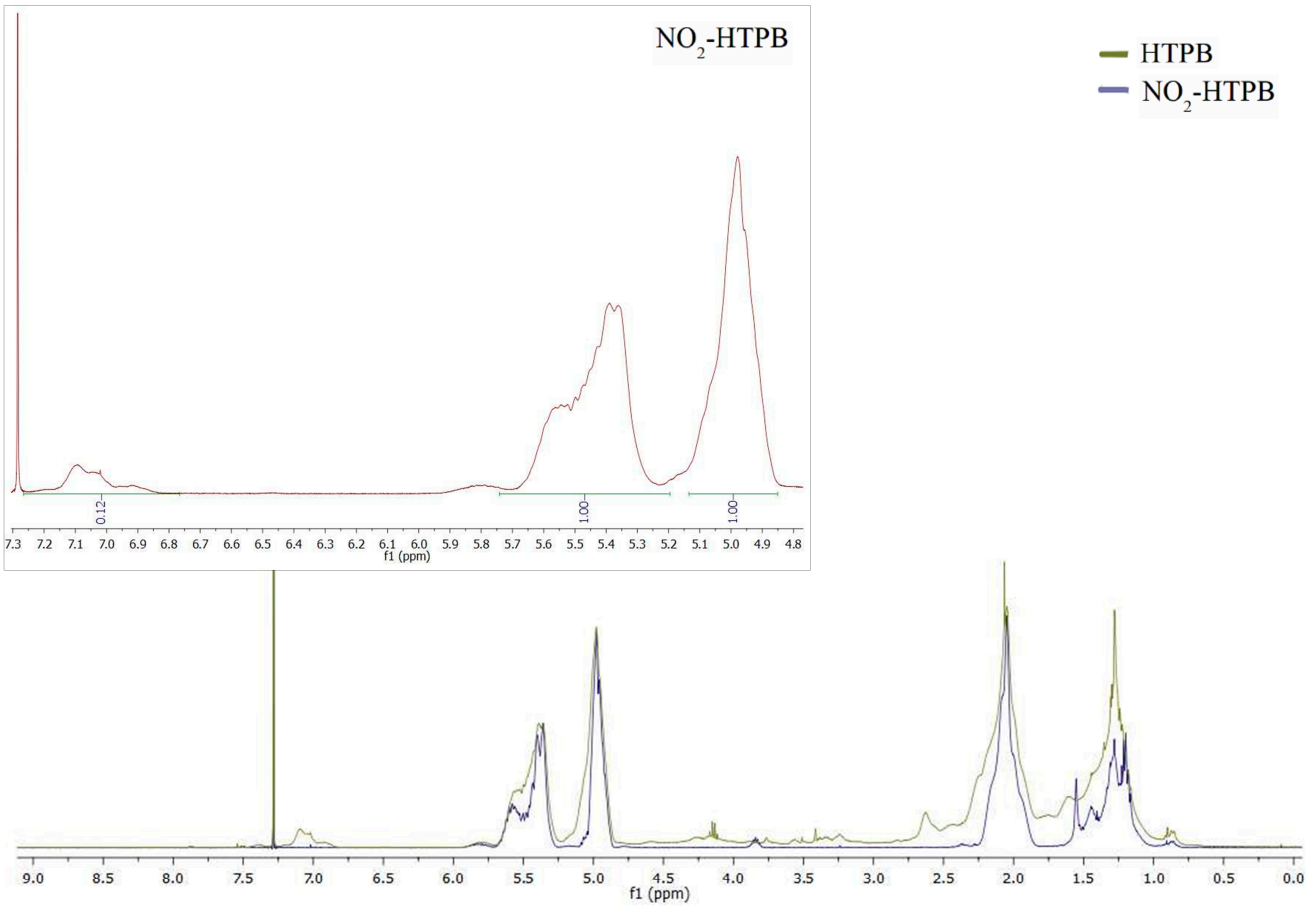

Figure 3. ^{1}H NMR spectra of starting HTPB and synthesized nitro-HTPB.

The use of ^{1}HNMR for the measurement and calculation of nitro functionalization of HTPB is expensive, time-consuming, and particularly impractical on an industrial scale. At the same time the above-discussed FTIR analysis provides a possibility to perform a ratiometric evaluation for the quantitative detection of HTPB nitro functionality in which the percentage of nitro functionalization could be determined from the ratio between intensities of the characteristic peaks for nitro groups at 1523 cm^{-1} and alkene fragments at 1640 cm^{-1}. Moreover, this measurement is based on a relatively inexpensive and rapid ATR technique, suitable for industrial monitoring.

In order to prove the concept that FTIR analysis is a useful tool for quantitative control in HTPB nitration, the changes in the FTIR spectra at 1523 cm^{-1} relative to the peak at 1640 cm^{-1} of nitro-HTPB with different percentages of nitro functionality were investigated (Figure 4). On the basis of the ratio between examined peak intensities at 1523 cm^{-1} and 1640 cm^{-1} as a function of HTPB nitro functionality (calculated according to the respective NMR spectra) a calibration plot was constructed. As is shown in Figure 4B, in the studied interval of nitro functionality, the resulting calibration curve revealed an excellent linear fit with R^2 = 0.99354. The linear response is preferable in chemical analysis; therefore, this finding suggests the great potential of FTIR in the ratiometric measurement and determination of the nitro functionality in nitro-HTPB. Also, the ratiometric analysis is of particular interest, because the ratiometric response allows internal calibration which

compensates instrumental factors (such as fluctuations in light source) and does not depend on sample concentration [31].

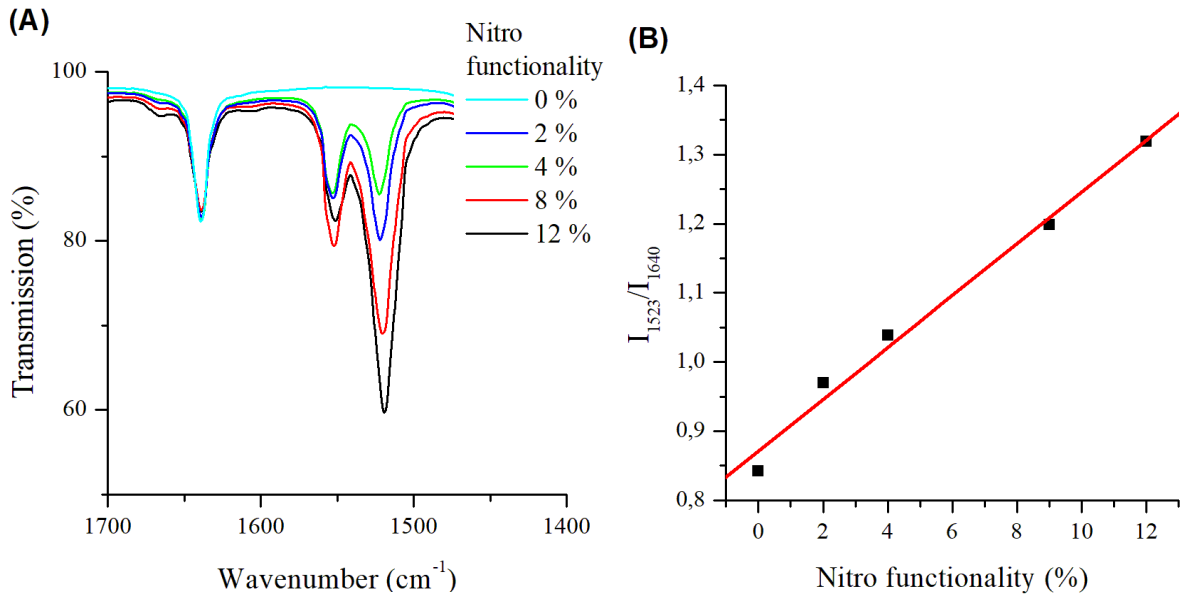

Figure 4. Changes in FTIR spectra of nitrated HTPB with different nitro functionality (**A**) and changes in ratio between intensity at 1523 cm^{-1} and constant alkenes signal at 1640 cm^{-1} (**B**) according to nitro functionality.

The average molecular weights of starting and nitrated HTPB were measured by GPC as 4810 g/mol and 5375 g/mol, respectively. The observed increase in molecular weight of 565 g/mol in nitro-HTPB compared to the initial compound is of the same order of magnitude as previously reported data. For example, in the works by Ghayeni et al. the terminated average molecular weight of HTPB increased from 2550 g/mol to 2780 g/mol [28] and 2586 g/mol to 2730 g/mol [25] after nitration, which gives an approximately two times lower increase in molecular weight compared to the present work; however, it was based on a two times lower percentage of nitro functionality. Also, the work by Pant et al. [29] showed an increase in average molecular weight with 543 g/mol after nitro functionalization of HTPB with 10–15% nitro content, which is very close to the obtained results in this work. The determined specific gravity at 25 °C of HTPB increased from 0.89 to 1.14 after nitration, which is slightly higher compared to the value of 1.12 of nitro-HTPB with similar nitro functionality reported by Pant et al. [29]

The DSC analysis was performed with a temperature rate of 10 °C/min in two general ways. First, the samples were examined at low temperature from −70 °C to room temperature in order to determine glass transition, and second, from room temperature to 400 °C. The observed glass transition temperature (Tg) curves of nitrated and unmodified HTPB are presented in Figure 5. As expected, due to the incorporation of polar nitro groups, the synthesized nitro-HTPB showed higher Tg = −27 °C compared to the obtained Tg = −46 °C for the starting HTPB. The calculated difference between the Tg of both products is 19 °C, which is a little higher in comparison to the previous report by Pant et al. for nitrated HTPB with similar nitro functionality, where this difference is 14 °C [29]. However, in the work by Pant et al. the initial HTPB is more linear than the compound used herein and logically showed lower temperatures of glass transition before (Tg = −76 °C) and after (Tg = −61 °C) nitration.

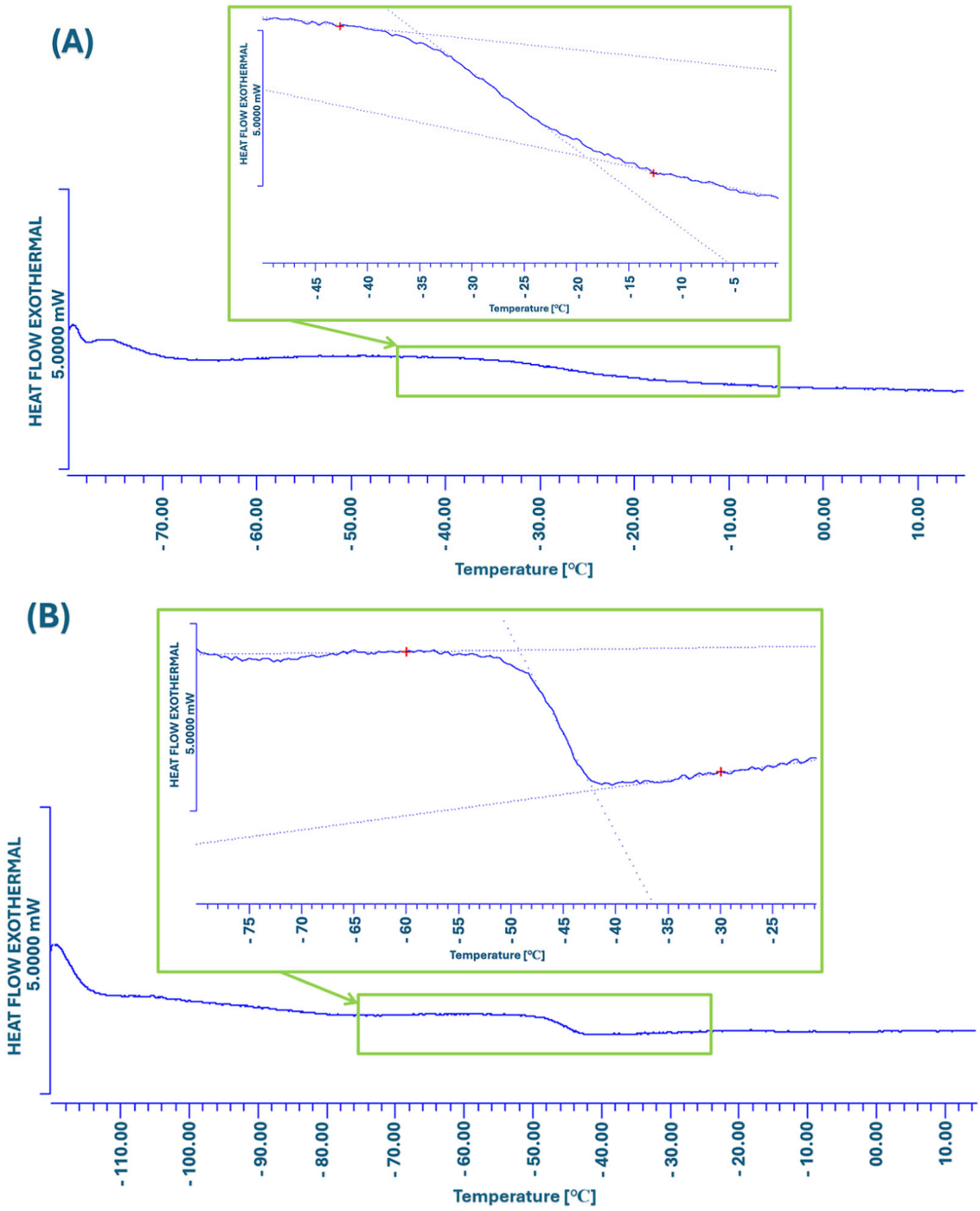

Figure 5. DSC analysis of synthesized nitro-HTPB (**A**) and starting HTPB (**B**) from −70 °C to 10 °C.

A DSC thermogram of nitrated HTPB heated at 10 °C/min from room temperature to 400 °C is depicted in Figure 6. The illustrated curve reveals an initial exothermic decomposition in the range of 140–280 °C with the peak temperature at 226 °C accompanied with heat release of 856 J/g. This result is consistent with the data for nitrated HTPB in which the exothermic decomposition peak was in the range of 220–232 °C [25,28,29].

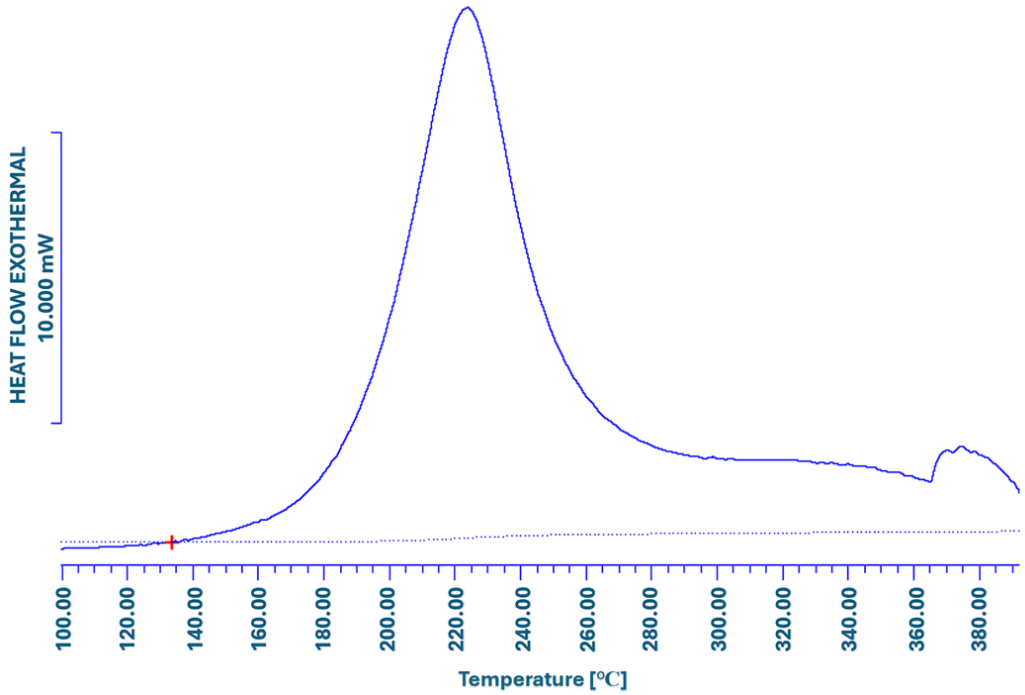

Figure 6. DSC analysis of the nitrated HTPB heated at 10 °C/min to 400 °C.

For a better understanding of the above obtained data for HTPB and nitrated HTPB, a summary is provided in Table 1.

Table 1. Properties of HTPB and NO_2-HTPB.

	HTPB	**NO_2-HTPB**
Average molecular weights	4810 g/mol	5375 g/mol
Specific gravity	0.89	1.14
Glass transition temperature	−76 °C	−27 °C

4. Conclusions

In conclusion, this work extends the classic nitration of HTPB using nitryl iodide (NO_2I) as a nitrating agent by introducing accelerated reaction conditions under ultrasonication. As a result of the applied sonic energy the reaction time was drastically reduced from the classic 96–144 h to only 20 h. The final compound showed 12% nitro functionality, which is comparable with the other highly efficient syntheses. The data obtained from FTIR, ^{1}HNMR, DSC, and GPC analyses were consistent with the reports about nitrated HTPB and clearly illustrated the absence of any ultrasonic influence on the produced nitro-HTPB. Also, it was revealed that the FTIR analysis can serve as fast, inexpensive, and reliable ratiometric method for determining HTPB nitro functionality, offering a practical alternative to the less convenient classical NMR method.

The results presented here could be seen as a contribution to the development of applied nitro chemistry and will support the rapid synthesis and characterization of nitrated HTPB.

Author Contributions: Conceptualization, M.B. and N.G.; investigation, V.B., S.Y., N.R., and D.G.; methodology, D.G. and N.G.; supervision, M.B. and N.G.; visualization, V.B. and N.R.; writing—original draft, M.B. and N.G.; writing—review and editing, S.Y. and N.G. All authors have read and agreed to the published version of the manuscript.

Funding: This study is funded by the European Union—NextGenerationEU, through the National Recovery and Resilience Plan of the Republic of Bulgaria, project № BG-RRP-2.004-0002, "BiOrgaMCT".

Institutional Review Board Statement: Not applicable.

Informed Consent Statement: Not applicable.

Data Availability Statement: The original contributions presented in this study are included in the article. Further inquiries can be directed to the corresponding author.

Acknowledgments: This work is developed as part of contract No.: BG-RRP-2.004-0002-C01, Laboratory of Organic Functional Materials (Project BiOrgaMCT), Procedure BG-RRP-2.004, "Establishing of a network of research higher education institutions in Bulgaria". Also, the authors are grateful to the Project BG05M2OP001-1.001-0008 National Centre for Mechatronics and Clean Technologies, and to Laboratory L2 "Bio-Mechatronics and micro/nano engineering for mechatronic technologies, elements and systems", Section S4 "Biomimetic mechatronic systems", and Project № 403-10, 2025, Synthesis and characterization of "green" high-energy materials, Scientific research sector, UCTM.

Conflicts of Interest: The authors declare no conflicts of interest.

References

1. Zhang, Q.; Shu, Y.; Liu, N.; Lu, X.; Shu, Y.; Wang, X.; Mo, H.; Xu, M. Hydroxyl Terminated Polybutadiene: Chemical Modification and Application of These Modifiers in Propellants and Explosives. *Cent. Eur. J. Energ. Mater.* **2019**, *16*, 153–193. [CrossRef]
2. Ashrafi, M.; Dehnavi, M.A.; Fakhraian, H. Synthesis, Characterization and Properties of Nitropolybutadiene as Energetic Plasticizer for NHTPB Binder. *Propellants Explos. Pyrotech.* **2017**, *42*, 269–275. [CrossRef]
3. Qin, P.; Zhang, X.; Jiang, K.; Cheng, J. Constant Strain Aging Model of HTPB Propellant Involving Thermal–Mechanical Coupled Effects. *Aerospace* **2025**, *12*, 589. [CrossRef]
4. Huang, Y.; Chang, K.; Yao, J.; Guo, X.; Shen, C.; Yan, S. Effect of Fluoroalcohol Chain Extension Modified HTPB Binder on the Combustion Performance of Aluminized Propellants. *Crystals* **2024**, *14*, 258. [CrossRef]
5. Saha, S.; Patel, J.; Bhattacharjee, A.; Chowdhury, A.; Kumbhakarna, N. Experimental and computational study on the decomposition mechanisms of cured hydroxyl-terminated polybutadiene grafted with nitro and tetrazole groups. *Combust. Flame* **2025**, *281*, 114431. [CrossRef]
6. Aljafree, N.; Norrrahim, M.; Samsuri, A.; Wan Yunus, W.M.Z. Environmental Impact and Sustainability of Nanocellulose-Based Nitrated Polymers in Propellants. *RSC Adv.* **2025**, *15*, 24167. [CrossRef]
7. Zhang, X.; Deng, Z.; Xu, W.; Jiang, L.; Xu, H.; Tang, Q.; Zheng, Q.; Li, J. Influence of Process Aids on Solid–Liquid Interfacial Properties of Three-Component Hydroxyl-Terminated Polybutadiene Propellants. *Polymers* **2025**, *17*, 286. [CrossRef] [PubMed]
8. Kim, H.-C.; Moon, S.-J.; Kwon, Y.-R.; Moon, S.; Kim, D.; Kim, D.-H. Novel Glycidyl Carbamate Functional Epoxy Resin Using Hydroxyl-Terminated Polybutadiene. *Polymers* **2024**, *16*, 3107. [CrossRef] [PubMed]
9. Guo, Q.; Wang, J.; Li, Y.; Artiaga, R. The Synergistic Effect of Fe-Based MOFs and HTPB on AP Decomposition in Solid Propellants. *Solids* **2025**, *6*, 27. [CrossRef]
10. Dou, J.; Xu, M.; Tan, B.; Lu, X.; Mo, H.; Wang, B.; Liu, N. Research Progress of Nitrate Ester Binders. *FirePhysChem* **2023**, *3*, 54–77. [CrossRef]
11. Jouini, M.; Abdelaziz, A.; Trache, D.; Tarchoun, A.; Amokrane, S.; Benzetta, A.; Mezroua, A. HTPB Propellant Binder Supplemented with Nitro Potato Starch: Formulation, Characterization, and Thermal Decomposition Behavior. *FirePhysChem* **2024**, *4*, 211–215. [CrossRef]
12. Wang, Q.; Wang, L.; Zhang, X.; Mi, Z. Thermal Stability and Kinetics of Decomposition of Nitrated HTPB. *J. Hazard. Mater.* **2009**, *172*, 1659–1664. [CrossRef]
13. Runtu, K.; Hafizah, M.; Triharjanto, R.; Navalino, D. Study of Burning Rate Characteristics of Composite Propellant Based on Nitrated Hydroxyl Terminated Polybutadiene (NHTPB) Binder. *UIJRT* **2022**, *3*, 100–104.
14. Saha, S.; Bhattacharjee, A.; Bhagat, S.; Kumar, A.; Pawar, R.; Singh, S.; Namboothiri, I.; Chowdhury, A.; Kumbhakarna, N. Theoretical, Structural, and Thermal Aspects of Nitro-HTPB as a Prospective Energetic Binder—A Detailed Computational and Experimental Analysis. *Mater. Today Commun.* **2024**, *38*, 107892. [CrossRef]
15. Jouini, M.; Abdelaziz, A.; Tarchoun, A.; Rahamnia, F.; Bekhouche, S.; Pal, Y.; Pang, W.; Trache, D. Enhancing Energetic Features of HTPB Binder Through Nitro-Functionalization and Nitrocellulose Doping. *FirePhysChem* **2025**, *in press*. [CrossRef]
16. Huang, Z.Z.; Nie, H.; Zhang, Y.; Tan, L.; Yin, H.; Ma, X. Migration Kinetics and Mechanisms of Plasticizers, Stabilizers at Interfaces of NEPE Propellant/HTPB Liner/EPDMInsulation. *J. Hazard. Mater.* **2012**, *229–230*, 251–257. [CrossRef] [PubMed]

17. Yang, L.; Mei, L.; La, Y.; Liao, L.; Fu, Y. Molecular Dynamics Simulation on Compatibility and Glass Transition Temperature of HTPB/Plasticizer Blends. *Adv. Mater. Res.* **2013**, *718–720*, 136–140. [CrossRef]
18. Akwi, F.M.; Watts, P. Continuous Flow Chemistry: Where Are We Now? Recent Applications, Challenges and Limitations. *Chem. Commun.* **2018**, *54*, 13894–13928. [CrossRef] [PubMed]
19. Zheng, Z.; Liang, X.; Zhou, X.; Zhu, R.; Liu, F. Research Progress on Continuous-Flow Nitrification Technology and Equipment. *Pharmaceut. Front.* **2025**, *7*, 77–90. [CrossRef]
20. Krishnan, P.; Ayyaswamy, K.; Nayak, S. Hydroxy Terminated Polybutadiene: Chemical Modifications and Applications. *J. Macromol. Sci. A* **2013**, *50*, 128–138. [CrossRef]
21. Colclough, M.; Paul, N. Nitrated Hydroxy-Terminated Polybutadiene: Synthesis and Properties. In *Nitration*; ACS Symposium Series; American Chemical Society: Washington, DC, USA, 1996; Volume 623, pp. 97–103.
22. Yoon, S.; Lee, S.; Lee, J. Comprehensive Review on Post-Polymerization Modification of Hydroxyl-Terminated Polybutadiene (HTPB). *Elastomers Compos.* **2024**, *59*, 108–120.
23. Colclough, M.; Desai, H.; Millar, R.; Paul, N.; Stewart, M.; Golding, P. Energetic Polymers as Binders in Composite Propellants and Explosives. *Polym. Adv. Technol.* **1993**, *5*, 554–560. [CrossRef]
24. Chien, J.; Kohara, T.; Lillya, C.; Sarubbi, T.; Su, B.-H. Phase Transfer-Catalyzed Nitromercuration of Diene Polymers. *J. Polym. Sci. Polym. Chem. Ed.* **1980**, *18*, 2723–2729. [CrossRef]
25. Ghayeni, H.; Razeghi, R.; Olyaei, A. Synthesis and Characterization of Nitro-Functionalized Hydroxyl-Terminated Polybutadiene Using N-Iodosuccinimide. *Polym. Bull.* **2020**, *77*, 4993–5004. [CrossRef]
26. Abusaidi, H.; Ghorbani, M.; Ghaien, H. Development of Composite Solid Propellant Based on Nitro-Functionalized Hydroxyl-Terminated Polybutadiene. *Propellants Explos. Pyrotech.* **2017**, *42*, 671–675. [CrossRef]
27. Azazy, A.; Saleh, A.; Aly, W.; Elbeih, A.; Hussein, A.K.; Elshenawy, T.; Abdelhafiz, M.; Wafy, T.; Zaki, M.; Ahmed, H. Enhancing the Propulsion Characteristics of Rockets by Adding the Energetic Nitro-Hydroxyl-Terminated Polybutadiene (NHTPB) in the Propellant Compositions. *IOP Conf. Ser. Mater. Sci. Eng.* **2021**, *1172*, 012032. [CrossRef]
28. Ghayeni, H.; Razeghi, R.; Kazemi, F.; Olyaei, A. An Efficient Synthesis, Evaluation of Parameters and Characterization of Nitro-Hydroxyl-Terminated Polybutadiene (Nitro-HTPB). *Propellants Explos. Pyrotech.* **2018**, *43*, 574–582. [CrossRef]
29. Pant, C.; Santosh, M.; Banerjee, S.; Khanna, P. Single Step Synthesis of Nitro-Functionalized Hydroxyl-Terminated Polybutadiene. *Propellants Explos. Pyrotech.* **2013**, *35*, 748–753. [CrossRef]
30. Alavi Nikje, M.M.; Mozaffari, Z. Chemoselective Epoxidation of Hydroxyl-Terminated Polybutadiene (HTPB) Using In-Situ Generated Dimethyl Dioxirane (DMD). *Des. Monomers Polym.* **2007**, *10*, 67–77. [CrossRef]
31. Demchenko, A. Practical Aspects of Wavelength Ratiometry in the Studies of Intermolecular Interactions. *J. Mol. Struct.* **2014**, *1077*, 51–67. [CrossRef]